Available online at www.sciencedirect.com
ScienceDirect
International Journal of Thermal Sciences 47 (2008) 1630–1638
International Journal of Thermal Sciences
www.elsevier.com/locate/ijts

# Laminar and turbulent natural convection combined with surface thermal radiation in a square cavity with a glass wall

J. Xamán [a,*], J. Arce [a,b,1], G. Álvarez [a], Y. Chávez [a]

[a] *Centro Nacional de Investigación y Desarrollo Tecnológico (CENIDET-DGEST-SEP), Prol. Av. Palmira S/N Col. Palmira, Cuernavaca, Morelos, CP 62490, Mexico*

[b] *Centro de Investigación en Energía (CIE-UNAM), Priv. Xochicalco S/N Col. Centro, Temixco, Morelos, CP 62580, Mexico*

Received 24 August 2007; received in revised form 15 December 2007; accepted 3 January 2008

Available online 4 March 2008

**Abstract**

A two-dimensional numerical study of combined heat transfer (laminar and turbulent natural convection, surface thermal radiation and conduction) in a square cavity with a glass wall is presented. The cavity is modeled as one vertical isothermal wall, two horizontal adiabatic walls and one vertical glass wall. Numerical results in the cavity are obtained by means of a control volume approach where the conditions are set as: 21 °C uniform temperature in the isothermal wall, 35 °C outside ambient temperature and 750 W/m$^2$ constant direct normal solar irradiation over the glass wall. The Rayleigh number was varied between the range $10^3 \leqslant Ra \leqslant 10^{12}$. Results show that the flow pattern is not symmetric due to the combined effect of non-isothermal glass wall and radiative exchange inside the cavity. A correlation for the total Nusselt number was obtained for both laminar and turbulent flow considering conjugate heat transfer.


*Keywords:* Combined heat transfer; Turbulent natural convection; Radiative exchange

## 1. Introduction

Due to its many engineering applications and the impact on flow structure and heat transfer processes in double pane windows, solar collectors, building insulation, ovens and rooms, natural convection inside enclosures has been a very important research topic. Previous studies on laminar and turbulent natural convection in a rectangular enclosure were mainly focused on flow and heat transfer inside the fluid region with temperature gradient [1–6]. Nevertheless, they were carried out neglecting radiation heat transfer, despite the fact this phenomenon occurs in numerous engineering applications such as environment inside buildings. Many studies on laminar and turbulent natural convection heat transfer in a rectangular enclosure are carried out including radiation [7–11]. On the other hand, very few studies deal with the effect that a semitransparent wall in a cavity has over conjugate natural convection and radiation. Behnia et al. [12] consider a cavity with one glass sheet wall; numerical results are presented for a variety of Rayleigh numbers in the range $10^4 < Ra < 3 \times 10^5$. Behnia et al. conclude that in general terms, the external convection weakens the internal circulation, radiation strengthens it, and in combination the overall effect is a strengthening of the internal circulation. Kwon et al. [13] present a numerical study of combined laminar natural convection and radiation in a rectangular enclosure with a transparent window. Their results show that temperature distributions of adiabatic walls increase with the transmittance of the transparent window; however, those for solar radiation are higher than those for surface radiation and pure natural convection. Álvarez et al. [14] publish results of a transient computational model for combined laminar natural convection, conduction and radiation in a square cavity. The cavity is modeled with a vertical glass wall with film coating. Results show that there is a diminished convective regime due to the influence of the radiative exchange. The authors show that the total

* Corresponding author. Tel.: +52 (777) 3 62 77 70; fax: +52 (777) 3 62 77 95.

*E-mail addresses:* jxaman@cenidet.edu.mx (J. Xamán), jearl@cie.unam.mx (J. Arce), gaby@cenidet.edu.mx (G. Álvarez), ycchena@cenidet.edu.mx (Y. Chávez).

[1] Tel.: + 52 (55) 5622-9813; fax: + 52 (55) 5622-9814.

1290-0729/$ – see front matter 
doi:10.1016/j.ijthermalsci.2008.01.012

**Nomenclature**

| | | |
|---|---|---|
| $dF_{dA_j-dA_k}$ | view factor between elements $j$–$k$ | |
| $C_p$ | specific heat | $J\,kg^{-1}\,K^{-1}$ |
| $C_{1\varepsilon}$, $C_{2\varepsilon}$, $C_{3\varepsilon}$, $C_\mu$ | constants of the turbulence model | |
| $g^*$ | gravitational acceleration | $9.81\ m\,s^{-2}$ |
| $G$ | solar radiation | $W\,m^{-2}$ |
| $G_k$ | buoyancy production/destruction of kinetic energy | |
| $h_{ext}$ | convective heat transfer coefficient at the outside glass wall | $W\,m^{-2}\,K^{-1}$ |
| $H$ | height of the cavity | m |
| $L$ | thickness of the glass | m |
| $Nu$ | Nusselt number | |
| $P$ | pressure | Pa |
| $P_K$ | turbulence kinetic energy production | |
| $Pr$ | Prandtl number ($\nu/\alpha$) | |
| $q$ | heat flux | $W\,m^{-2}$ |
| $Ra$ | Rayleigh number ($g^*\beta\Delta T H^3/\nu\alpha$) | |
| $s_g$ | extinction coefficient | $m^{-1}$ |
| $T$ | temperature | K |
| $T^*$ | dimensionless temperature ($T - T_2/T_{g-\max} - T_2$) | |
| $T_2$ | cold wall temperature | K |
| $T_4$ | average temperature of the glass wall | K |
| $T_0$ | reference temperature [$(T_4 + T_2)/2$] | K |
| $u$, $v$ | dimensional horizontal and vertical velocities | $m\,s^{-1}$ |
| $u_{ref}$ | reference velocity $(g^*\beta(T_{g\text{-}\max} - T_2)H)^{1/2}$ | $m\,s^{-1}$ |
| $u^*$, $v^*$ | dimensionless horizontal and vertical velocities, $u/u_{ref}$, $v/u_{ref}$ | |
| $W$ | length of the cavity | m |
| $x$, $y$ | dimensional coordinates | m |
| $x^*$, $y^*$ | dimensionless coordinates, $x/H$, $y/H$ | |

*Greek symbols*

| | | |
|---|---|---|
| $\alpha$ | thermal diffusivity | $m^2\,s^{-1}$ |
| $\alpha^*$ | absorptivity | |
| $\beta$ | thermal expansion coefficient | $K^{-1}$ |
| $\Delta T$ | temperature difference $(T_4 - T_2)$ | K |
| $\varepsilon$ | rate of dissipation of $\kappa$ | $m^2\,s^{-3}$ |
| $\varepsilon^*$ | emissivity | |
| $\kappa$ | turbulence kinetic energy | $m^2\,s^{-2}$ |
| $\lambda$ | thermal conductivity | $W\,m^{-1}\,K^{-1}$ |
| $\mu_t$ | turbulent viscosity | $kg\,m^{-1}\,s^{-1}$ |
| $\nu$ | kinematic viscosity | $m^2\,s^{-1}$ |
| $\rho$ | density | $kg\,m^{-3}$ |
| $\rho^*$ | reflectivity | |
| $\sigma$ | Stefan–Boltzmann constant, $5.670 \times 10^{-8}$ | $W\,m^{-2}\,K^{-4}$ |
| $\sigma_T$ | turbulent Prandtl number | |
| $\tau^*$ | transmissivity | |

*Subscripts*

| | |
|---|---|
| $a$ | air |
| amb | ambient |
| cond | conductive |
| conv | convective |
| $g$ | glass wall |
| in | inlet |
| out | outlet |
| rad | radiative |
| total | total quantities |

energy transferred through the glass/solar control coating system is lower than the one that uses clear glass. Recently, Xamán et al. [15] determined the influence of the semitransparent glazing with and without SnS–$Cu_xS$ solar control coating on turbulent natural convection in a square cavity, where the effects of surface thermal radiation are neglected. Results show that direct solar energy transmittance of the semitransparent glazing with film coating is much lower than the one without solar control coating, thus the total heat gain through the glazing with solar control coating would be lower than the one without solar control coating.

As it is shown in the literature review, detailed studies of fluid flow and conjugate heat transfer inside an enclosure with a glass wall are scarce due to its complexity, so more comprehensive studies are required. In this work we consider a detailed study of fluid flow and heat transfer by laminar and turbulent natural convection and surface thermal radiation in a square cavity with a glass wall. A Rayleigh number range from $10^3$ to $10^6$ and $10^9$ to $10^{12}$ were chosen for the heat transfer study in square cavity. The Rayleigh number is based on the difference of temperature between the vertical walls, using the mean temperature for the glass wall ($T_4$). Natural convection and surface thermal radiation equations were solved simultaneously using the finite volume method and the net radiation method. Flow and temperature patterns are discussed and values of the Nusselt number as a function of the Rayleigh number are presented.

## 2. Physical and mathematical model

The square cavity ($H = W$) is shown in Fig. 1. Two-dimensional flow is considered taking into account that the dimension in $z$ direction is much longer than the other two. The left surface of the cavity is an isothermal opaque wall at 21 °C ($T_2 = 294$ K); the top and bottom horizontal surfaces are considered adiabatic; the right surface is a glass conductive wall of 6 mm thickness. The incident solar radiation over the glass wall is assumed to be normal at the surface with a constant value of AM2 ($G = 750\ W/m^2$). The glass surface transmits, reflects and absorbs normal solar radiation flux. Absorbed solar radiation flux increases the glazing temperature and it is transferred by conduction to the inside and outside of the cavity. The glass wall as well as the opaque walls are considered gray, diffusive, radiation reflecting and emitting surfaces. The air flow inside the cavity is considered steady, radiatively non-participating in both laminar and turbulent regimes ($Pr = 0.71$). The Boussi-

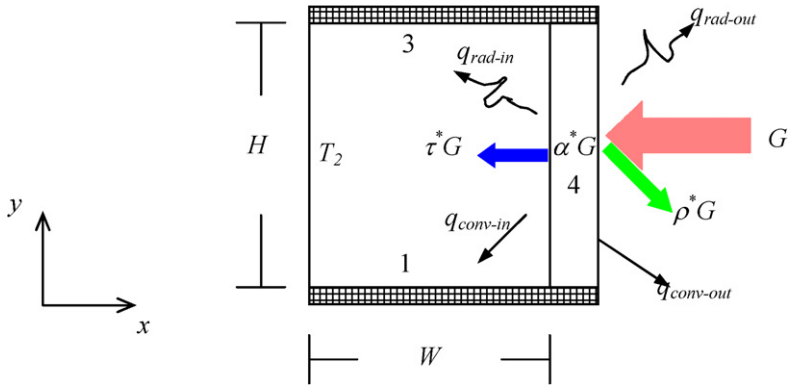


Fig. 1. Schematic representation of square cavity problem for the conjugate heat transfer analysis.

Table 1
Cavity widths used in calculations

| *Ra* (Laminar regime) | *W* (m) | *Ra* (Turbulent regime) | *W* (m) |
|---|---|---|---|
| $10^3$ | $6.98 \times 10^{-3}$ | $10^9$ | $6.98 \times 10^{-1}$ |
| $10^4$ | $1.50 \times 10^{-2}$ | $10^{10}$ | 1.50 |
| $10^5$ | $3.24 \times 10^{-2}$ | $10^{11}$ | 3.24 |
| $10^6$ | $6.98 \times 10^{-2}$ | $10^{12}$ | 6.98 |

nesq approximation is assumed with constant thermophysical properties and optical properties are the integrated spectrum values. In order to obtain a higher *Ra*, the cavity dimensions were increased. Table 1 shows the relationship between width of the cavity and *Ra*, as *Ra* increases from $10^3$ to $10^{12}$.

### 2.1. Turbulent natural convection model

The governing equations for turbulent natural convection in the square cavity with a semitransparent wall are the average equations of mass, momentum and energy. The equations are expressed in tensor form as:

$$\frac{\partial(\rho u_i)}{\partial x_i} = 0 \tag{1}$$

$$\frac{\partial(\rho u_j u_i)}{\partial x_j} = -\frac{\partial P}{\partial x_i} + \frac{\partial}{\partial x_j}\left(\mu \frac{\partial u_i}{\partial x_j} - \rho \overline{u_i' u_j'}\right) - \rho\beta(T - T_0) g_i^* \tag{2}$$

$$\frac{\partial(\rho u_i T)}{\partial x_i} = \frac{\partial}{\partial x_i}\left(\frac{\lambda}{C_p}\frac{\partial T}{\partial x_i} - \rho \overline{u_i' T'}\right) \tag{3}$$

The above equations system is not complete because of the presence of the Reynolds stress tensor ($\rho \overline{u_i' u_j'}$) in the momentum equation and the turbulent heat vector ($\rho \overline{u_i' T'}$) in the energy equation. In the Eddy Viscosity Model (EVM) the Reynolds stress tensor is modeled through the Boussinesq hypothesis as:

$$\rho \overline{u_i' u_j'} = -\mu_t\left(\frac{\partial u_i}{\partial x_j} + \frac{\partial u_j}{\partial x_i}\right) + \frac{2}{3}\rho\kappa\delta_{ij} \tag{4}$$

The High Reynolds Number model (HRN) establishes that the turbulent viscosity ($\mu_t$) can be obtained as:

$$\mu_t = C_\mu \frac{\rho\kappa^2}{\varepsilon} \tag{5}$$

where $C_\mu$ is a constant. The turbulent heat vector is modeled as follow

$$\rho \overline{u_i' T'} = -\frac{\mu_t}{\sigma_T}\frac{\partial T}{\partial x_i} \tag{6}$$

where $\sigma_T$ is the turbulent Prandtl number and $\delta_{ij}$ is the Kronecker deltas. The turbulent kinetic energy and the turbulent dissipation of kinetic energy can be obtained using its corresponding transport equation:

$$\frac{\partial(\rho u_i \kappa)}{\partial x_i} = \frac{\partial}{\partial x_i}\left[\left(\mu + \frac{\mu_t}{\sigma_\kappa}\right)\frac{\partial \kappa}{\partial x_i}\right] + P_\kappa + G_\kappa - \rho\varepsilon \tag{7}$$

$$\frac{\partial(\rho u_i \varepsilon)}{\partial x_i} = \frac{\partial}{\partial x_i}\left[\left(\mu + \frac{\mu_t}{\sigma_\varepsilon}\right)\frac{\partial \varepsilon}{\partial x_i}\right] + \left[C_{1\varepsilon}(P_\kappa + C_{3\varepsilon}G_\kappa) - C_{2\varepsilon}\rho\varepsilon\right]\frac{\varepsilon}{\kappa} \tag{8}$$

where, $P_\kappa$ and $G_\kappa$ are the shearing production and the generation/destruction of buoyancy turbulent kinetic energy.

Velocity boundary conditions on the walls are zero and temperature boundary conditions are set as: the adiabatic horizontal walls (up and bottom), the left vertical wall is isotherm and heat transfer by conduction is considered at the glass wall (right wall), that is:

Bottom adiabatic wall (wall 1):

$$q_{\text{cond-1}} = -q_{\text{rad-1}} \tag{9}$$

Isothermal vertical wall (wall 2):

$$T(0, y, t) = T_2 \tag{10}$$

Upper adiabatic wall (wall 3):

$$q_{\text{cond-3}} = -q_{\text{rad-3}} \tag{11}$$

Glass vertical wall (wall 4):

$$q_{\text{cond-}g\text{-4}} = q_{\text{cond-4}} + q_{\text{rad-4}} \tag{12}$$

Where $q_{\text{cond-1}}$, $q_{\text{cond-3}}$ and $q_{\text{cond-4}}$ are the conduction heat transfer fluxes from the inner surface to the adjacent fluid on walls 1, 3 and 4, respectively. The terms $q_{\text{rad-1}}$, $q_{\text{rad-3}}$ and $q_{\text{rad-4}}$ are the net radiative heat transfer fluxes over the walls 1, 3 and 4. Finally, $q_{\text{cond-}g\text{-4}}$ is the heat flux by heat conduction through of the glass wall.

The boundary conditions and constant values for $\kappa - \varepsilon$ turbulence model are: $\kappa_w = 0.0$, $\varepsilon_w = \infty$, $C_\mu = 0.09$, $C_{1\varepsilon} = 1.44$, $C_{2\varepsilon} = 1.92$, $\sigma_\kappa = 1.0$, $\sigma_\varepsilon = 1.3$ and $C_{3\varepsilon} = \tanh|v/u|$ [16].

### 2.2. Conductive model of the glass wall

In order to obtain the temperature profile inside the glass wall ($L = 6$ mm), a differential energy balance was carried out. The model solution is used to determine the conductive heat flux ($q_{\text{cond-}g\text{-}4}$). The heat transfer equation for the differential element of the glass wall is given by:

$$\frac{\partial}{\partial x}\left[\frac{\lambda_g}{C_{pg}}\frac{\partial T_g}{\partial x}\right]+\frac{\partial}{\partial y}\left[\frac{\lambda_g}{C_{pg}}\frac{\partial T_g}{\partial y}\right]+\frac{1}{C_{pg}}\frac{d\Theta}{dx}=0 \tag{13}$$

where $\Theta$ is the attenuation energy function by absorption and scattering, which depends of the extinction coefficient ($s_g$) as follow [17]:

$$\Theta(x) = G\exp\left[-s_g(L-x)\right] \tag{14}$$

The boundary condition for the glass wall can be expressed as ($x = W + L$):

$$-\lambda_g\frac{\partial T_g}{\partial x} = h_{\text{ext}}[T_g - T_{\text{amb}}] + \sigma\varepsilon_g^*\left[T_g^4 - T_{\text{amb}}^4\right] \tag{15}$$

where $T_{\text{amb}}$ is the outside ambient temperature. In order to obtain the internal glass temperature ($T_g$), the following energy balance was carried out ($x = W$):

$$\lambda_g\frac{\partial T_g}{\partial x} = \lambda_a\frac{\partial T}{\partial x} + q_{\text{rad-4}} \tag{16}$$

The boundary conditions are adiabatic for the horizontal walls.

### 2.3. Radiative model

The net radiative method was used to calculate the resulting heat fluxes from the radiative exchange in the cavity [17]. The cavity surfaces are assumed to be opaque and diffuse except the vertical right wall which is a transparent wall. The radiative heat flux for the $j$th element on each wall is given by the following energy balance:

$$q_{\text{rad}_j}(x_j) = q_{\text{out}_j}(x_j) - q_{\text{in}_j}(x_j) \tag{17}$$

where the radiosity for the $j$th element is defined as:

$$q_{\text{out}_j}(x_j) = \varepsilon_j^*\sigma T_j^4(x_j) + \rho_j^* q_{\text{in}_j}(x_j) \tag{18}$$

the irradiation is given by:

$$q_{\text{in}_j}(x_j) = \sum_{k=1}^{m}\int_{A_k} q_{\text{out}_k}(x_k)\,\mathrm{d}F_{dA_j - dA_k} \tag{19}$$

where the summation over the $k$th surface element is to be taken for those elements over the boundary for which $j$ interacts radiatively.

### 2.4. Thermal parameters

The total heat transfer across the glass wall is given by the Nusselt numbers. The total heat transfer involves the contribution of the convective and radiative Nusselt numbers; thus, the total convective and radiative Nusselt numbers can be expressed as:

$$Nu_{\text{total}} = Nu_{\text{conv}} + Nu_{\text{rad}} \tag{20}$$

where:

$$Nu_{\text{conv}} = \frac{-\lambda_a}{q_{\text{cond}}}\int_0^H \frac{\partial T}{\partial x}\,\mathrm{d}y \tag{21}$$

$$Nu_{\text{rad}} = \frac{1}{q_{\text{cond}}}\int_0^H q_{\text{rad-4}}\,\mathrm{d}y \tag{22}$$

$$q_{\text{cond}} = \lambda_a(T_4 - T_2)/W \tag{23}$$

where $T_4$ is the average temperature on the inside surface of the glass wall.

## 3. Numerical procedure

The governing equations of the convective and conductive model described above are solved using a finite volume approach [18]. The equations are integrated over elementary control volumes located around each node of a grid. The position of the nodes is calculated using a stretching function so that the nodes are closer to each other near the walls of the cavity. The velocity components are calculated at a staggered grid while the scalar variables are calculated at the main grid (not-staggered). The convective terms are discretized applying the hybrid scheme and the diffusive terms with the central difference scheme. Coupling between the momentum and continuity equations is made with the SIMPLEC algorithm [19]. The algebraic equations system is solved applying the line by line method (LBL) with alternating direction implicit scheme (ADI). Furthermore, under-relaxation is introduced using the false transient strategy. If values in mass balance for every control volume as well as the residual values of the different equations are sufficiently low, overall convergence is obtained (typically $10^{-10}$). This convergence criterion assures an acceptable solution. A radiative balance at the walls is solved using an iterative approach in order to couple laminar and turbulent natural convection to surface thermal radiation effect at the boundaries. The view factors between the elements were determined by the Hottel's crossed string method; since the view factors are only a function of the geometry, their calculation was performed before the beginning of the main iteration procedure. The radiosity equations were solved by Simpson's rule [17].

The general procedure for the conjugate heat transfer in a cavity can be summarized in the following steps:

(1) Initial guess values of all variables ($u, v, T, \ldots, \varepsilon$) in the cavity were given.
(2) Eqs. (17)–(19) were computed in order to get the local radiative heat flux on the walls.
(3) The conductive model to obtain $q_{\text{cond-}g\text{-}4}$ was solved.
(4) The pressure-velocity ($u, v, p$) were calculated by the SIMPLEC algorithm.
(5) With the new calculated values of local radiative heat flux and velocity, the temperature ($T$), the turbulent kinetic energy ($\kappa$) and the turbulent dissipation of kinetic energy ($\varepsilon$) field in the cavity were obtained.
(6) A convergence criterion was applied, and

(7) the process was repeated iteratively until the convergence criterion was achieved.

The accuracy of the numerical results was verified through numerous tests based on the grid size effect. The used grids were from $61 \times 51$ to $101 \times 91$ with an increment of 10 computer nodes for $Ra = 10^{12}$ and surface thermal radiation coupled with turbulent natural convection flow was taken into account. Based on numerical calculations, the computational grid that gives grid independent solutions was $91 \times 81$ with a maximum deviation of 2% for the average Nusselt number. Therefore, a $91 \times 81$ grid was used for all cases herein considered. The discretization for the glass wall (6 mm) was always 10 nodes in the horizontal direction for all the meshes.

In order to validate the numerical code, the conjugate heat transfer problem by turbulent natural convection and surface thermal radiation in a square cavity with differentially heated vertical walls, reported by Velusamy et al. [9] was considered. Comparison of results was made with the following two cases:

*Case* 1 (the walls have an emissivity equal to 0.9, $T_4 = 328$ K, $T_2 = 318$ K and $Ra = 10^{11}$) and
*Case* 2 (the walls have an emissivity equal to 0.9, $T_4 = 348$ K, $T_2 = 298$ K and $Ra = 10^{11}$).

The comparison of results is analyzed for both cases in terms of the average Nusselt numbers (convective ($f$) and radiative ($r$) in the hot ($h$) and cold ($c$) wall). The maximum and minimum observed differences for case 1 are 3.14% for $Nu_{cf}$ and 0.11% for $Nu_{hr}$, respectively. In case 2, the maximum difference observed is 3.29% for $Nu_{cf}$ and the minimum difference is 0.10% for $Nu_{hr}$. However the differences for average total Nusselt numbers are 1 and 1.5% for cases 1 and 2, respectively.

## 4. Results and discussion

The parameters used to obtain the conjugate heat transfer results for the square cavity with a glass wall are described next. The cavity lengths considered in this work are shown in Table 1. The solar radiation incoming in a normal direction over the glass has a constant value of 750 W/m$^2$ (AM2). The glass thickness was 6 mm. The isothermal wall temperature was taken as 21 °C (294 K). The external conditions around the glass wall are: the external convection coefficient has a constant value of 6.8 W/m$^2$ K corresponding to a wind velocity of 3 m/s and the ambient temperature has a fixed temperature of 35 °C (308 K) (warm climates). The emissivity of the glass wall was 0.85. The optical properties of the glass were: 0.14 (absorptivity), 0.78 (transmissivity) and 0.08 (reflectivity). The remaining walls have an emissivity equal to 0.9.

### 4.1. Flow pattern results

Calculation results are graphically presented in Fig. 2. Streamlines Fig. 2(a) and isotherms Fig. 2(b) for different values of $Ra$ are shown. As can be seen on Fig. 2, flow is not symmetric contrary to the case where only natural convection heat transfer in a cavity is present [1]. For small values of $Ra$, a vortex appears at the center of the flow as a dominant characteristic of the flow. As the Rayleigh number increases, the vortex becomes elliptical ($Ra = 10^5$) and smaller as it tends to confine itself in the lower left corner of the cavity ($Ra = 10^6$). Rotation is counterclockwise. For high values of Rayleigh ($Ra \geqslant 10^9$), velocities at the centre of the cavity are smaller compared to those next to the boundaries, where the fluid moves faster. Further more; the absolute value of the horizontal component of velocity is much higher at the bottom of the cavity than at the top, this makes a long and thin vortex to form in the lower side of the cavity. This vortex makes the stratification in the upper side on the cavity to improve. This non-symmetric behavior of the flow pattern can be attributed to the variation of temperature on the glass wall combined with the radiative interchange at the inside of the cavity.

The isotherms patterns show the way the dominant heat transfer process changes as the Rayleigh number increases. For small values of $Ra$ the isotherms are quasi-verticals, due to heat transfer by conduction between the cold surface and the glass surface. As the isotherms deviate from the vertical shape, the heat transfer process changes from conduction to convection. As can be seen on Fig. 2(b), while the Rayleigh number increases, isotherms at the centre of the cavity are horizontal, and they become vertical over the boundary layer. Where turbulent flow only is present, the value of the median isotherm appears to be at the bottom of the cavity, contrary to the problem of natural convection in a cavity with isotherm walls [5], where the median isotherm is located at the center of the cavity, this is due to the velocity levels in the zone.

Fig. 3 shows the non-dimensional temperature profile at the median of the cavity, for different values of $Ra$. The profile for the fluid in laminar regime ($10^3 \leqslant Ra \leqslant 10^6$), shows an abrupt change in the heat transfer way from conductive regime to convective regime, it means, for a value of $Ra = 10^3$, the slope is 45°, after that, the profiles tend to be horizontal lines at the median of the cavity, as a consequence the temperature gradients become null along the with of the cavity, and temperature gradients can be found only inside the boundary layer for a $Ra > 10^6$ over the vertical walls. This allows stratification at the median of the cavity to be formed.

Fig. 4 shows the profiles for the non-dimensional velocity components at the median of the cavity. In the case study for laminar regime ($Ra \leqslant 10^5$), the horizontal velocity component has almost a symmetric behavior, the velocity decreases gradually close to the median of the cavity and a narrow boundary layer is developed along the walls. For $Ra = 10^6$, for $u^*$ a remarkable non-symmetrical behavior is already seen. For the case of turbulent flow, the horizontal velocity is totally asymmetric, and it value is higher at the lower side of the cavity than at the upper side, with an even narrower boundary layer than in the laminar regime. On the other hand, the vertical velocity component ($v^*$) shows a symmetric behavior. For values of $Ra > 10^6$, $v^*$ gets smaller outside the vertical boundary layer, and it tends to zero as the thermal stratification develops.

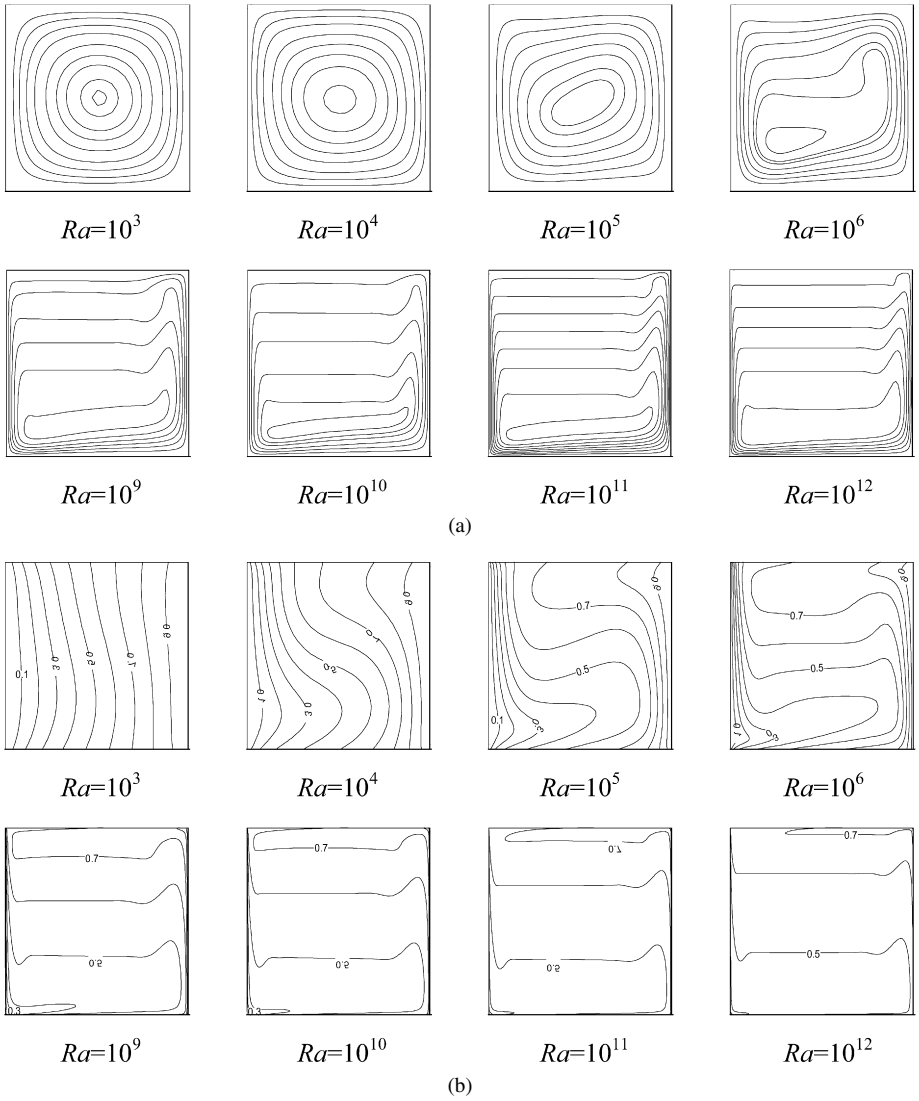


Fig. 2. Laminar and turbulent flow field at different *Ra* values: (a) streamlines and (b) isotherms.

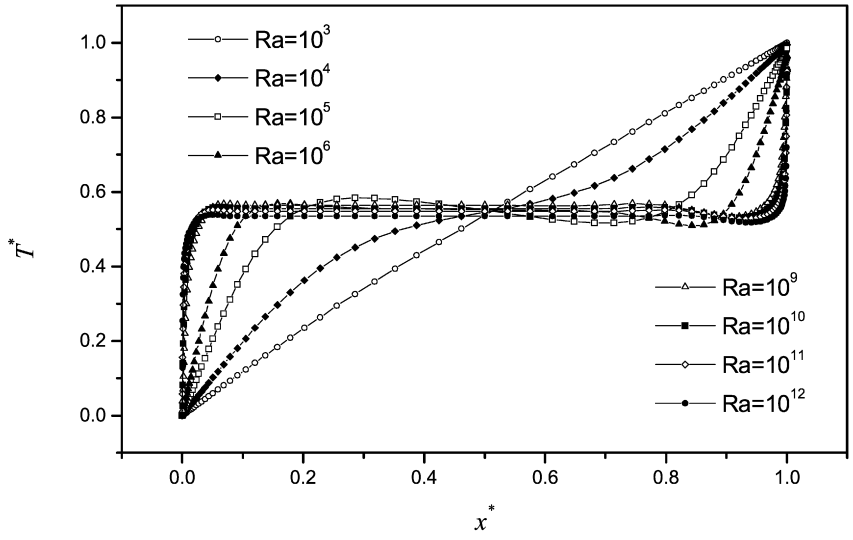


Fig. 3. Temperature distribution at mid-height of cavity for different *Ra* values.

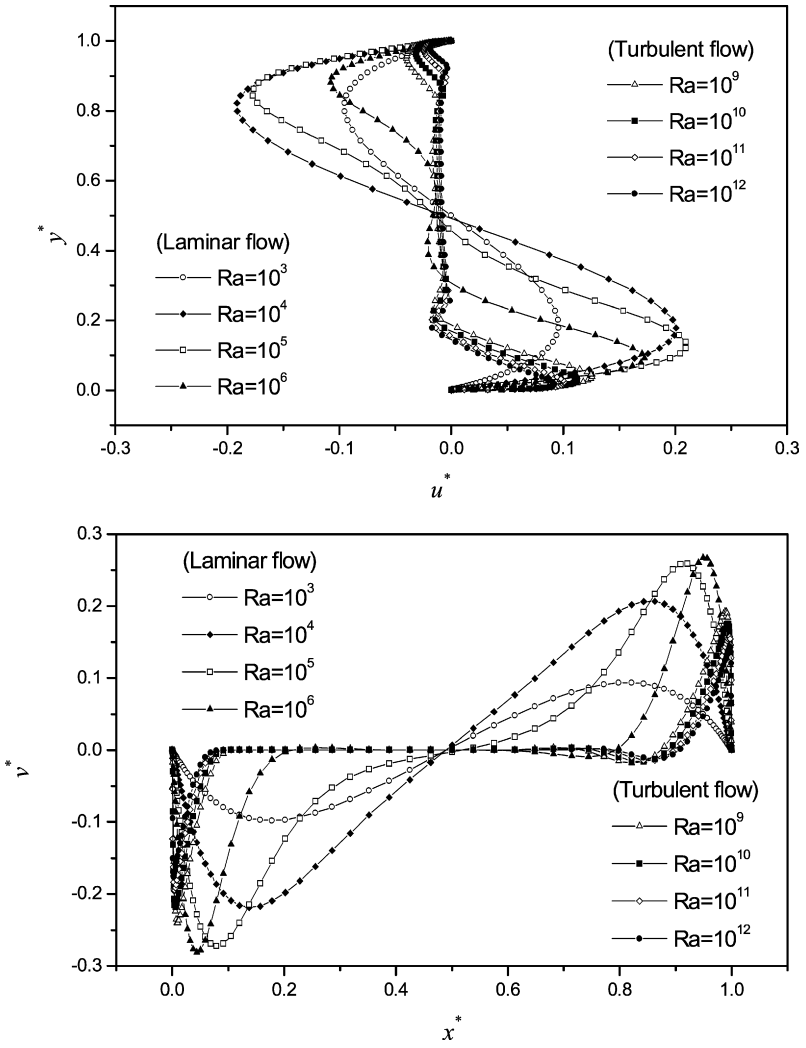


Fig. 4. Distribution of $u^*$- and $v^*$-velocity components respectively at mid-width and mid-height of cavity for different *Ra* values: (top) $u^*$-velocity and (bottom) $v^*$-velocity.

The non-symmetrical behavior of the horizontal velocity component with a consequent non-symmetrical flow pattern due to the combined effect of the heat transfer can be seen on Fig. 5, for Rayleigh numbers of $10^6$ and $10^{12}$. Three cases are taken into account in order to compare the effect of conjugated heat transfer over the velocity component.

*Case* 1: Convection-Radiation-Conduction; this case considers the three ways of heat transfer inside the cavity with a glass wall.

*Case* 2: Convection-Radiation; this case considers natural convection and radiative interchange inside the cavity, it means that the heat conduction effect through the glass wall is neglected, so this is replaced with an isothermal wall whose temperature value is the average of the one obtained in case 1, over the glass wall, and the emissivity is set the same as the glass wall.

*Case* 3: Conduction-Convection; this case considers natural convection inside the cavity and heat conduction through the glass wall; radiative interchange inside the cavity is neglected.

For both regimes (laminar and turbulent) it can be seen that in case 3 the velocity levels are lower and symmetric compared to the other two cases, this indicates that the radiative effect increases the velocity magnitude. The velocity component for case 2 is almost symmetric, the slight deviation on the symmetry is attributable to the emissivity of the walls whose values are not equal (emissivity on right side wall: 0.85, emissivity on the remaining walls: 0.90). For case 1 the velocity component is completely asymmetric, due to the combined effects of the radiative exchange inside the cavity and the heat conduction through the semitransparent wall.

### 4.2. Nusselt number

In order to visualize the under estimation of the heat transfer without the radiation effect, Table 2 shows the comparison of total Nusselt number between the case where the three modes of heat transfer are taken into account and the case where the radiative effect is neglected. From this comparison a maximum perceptual deviation of 28.88% for $10^3 \leqslant Ra \leqslant 10^6$ and 45.11% for $10^9 \leqslant Ra \leqslant 10^{12}$ can be observed. This result allows us to

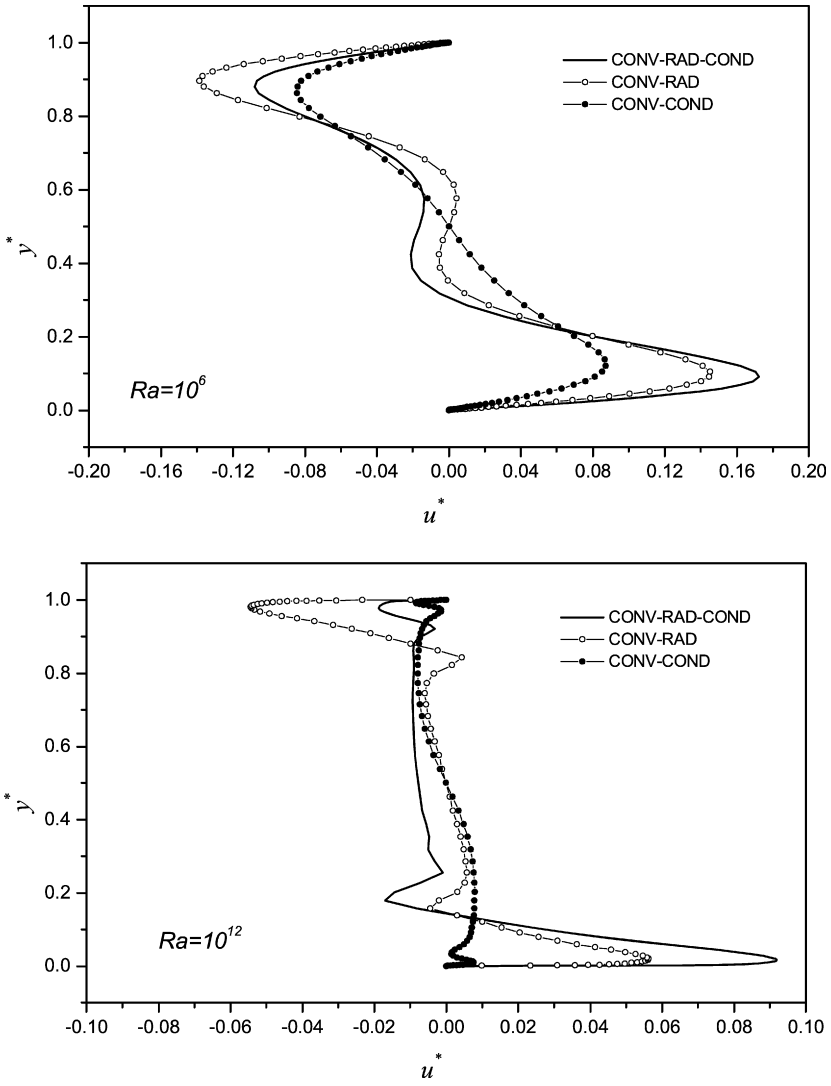


Fig. 5. Radiation and/or conduction effect on the natural convection for the horizontal velocity component at mid-width of cavity for different *Ra* values: (top) $10^6$ and (bottom) $10^{12}$.

Table 2
Radiative effect on the total Nusselt number ($Nu_{\text{total}}$)

| *Ra* | With radiation | Without radiation | Absolute differences (%) |
|---|---|---|---|
| $10^3$ | 1.45 | 1.04 | 28.28 |
| $10^4$ | 2.55 | 1.83 | 28.24 |
| $10^5$ | 5.11 | 3.77 | 26.22 |
| $10^6$ | 10.19 | 7.54 | 26.01 |
| $10^9$ | 94.95 | 52.12 | 45.11 |
| $10^{10}$ | 203.94 | 112.27 | 44.95 |
| $10^{11}$ | 439.39 | 253.31 | 42.35 |
| $10^{12}$ | 972.51 | 591.27 | 39.20 |

affirm that the radiative heat transfer should not be neglected in this type of problems, otherwise significant under estimations in the total heat transfer shall be found.

Fig. 6 shows the mean value of the total Nusselt number as a function of the Rayleigh for conjugate heat transfer in a cavity with a clear glass wall. It can be seen that the heat transfer has a linear behavior at a logarithmic scale for laminar and turbulent regime; this allows us to determine with certain accuracy an equation. The equation for calculating the mean value of the total Nusselt number was obtained by means of a minimum square regression, and it is given by: $Nu_{\text{total}} = 0.196Ra^{0.28}$ for the approximation laminar and $Nu_{\text{total}} = 0.088Ra^{0.34}$ for turbulent regime. The relations show a maximum percentage difference of 7.9% (laminar flow) and 8.8% (turbulent flow) respect to the numerical results.

## 5. Conclusions

Natural convection combined with surface thermal radiation in a square cavity with a glass wall have been numerically analyzed using a control volume approach. Calculations have been performed for both laminar and turbulent flow for a series of *Ra* up to $10^{12}$. The cavity was modeled as one vertical isothermal wall, two horizontal adiabatic walls and one vertical glass wall.

Results show that unlike the problem of natural convection in a cavity, flow patterns are not symmetric due to the combined effect of temperature variation over the glass wall and the radiative interchange inside the cavity. As the Rayleigh num-

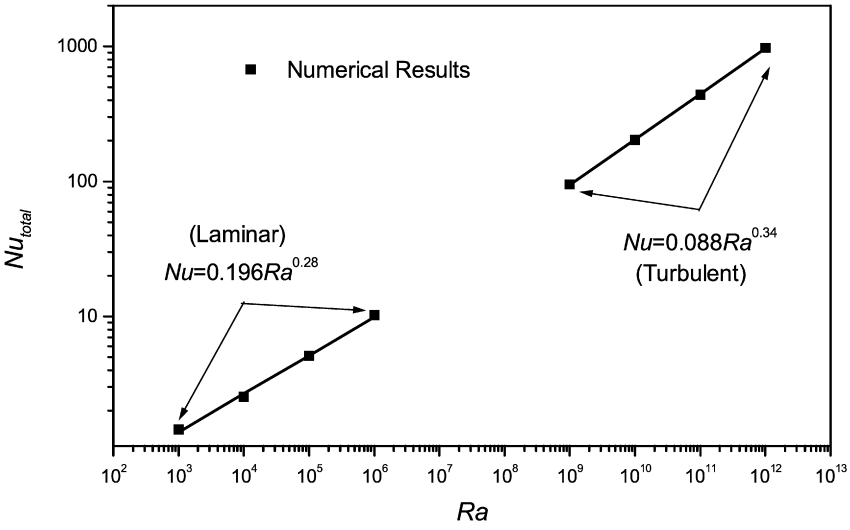


Fig. 6. Average total Nusselt number for $10^3 \leqslant Ra \leqslant 10^{12}$.

ber increases, velocity levels have their maximum value in the lower side of the cavity, causing the fluid to confine in its lowest region.

A total Nusselt number correlation as a function of Rayleigh number is presented for the studied cavities with a vertical glass wall for $10^3 \leqslant Ra \leqslant 10^{12}$. This correlation can be applied to determine the total heat transfer in rooms. Furthermore, this correlation can be used to supply information to commercial software, in order to determine the thermal loads in buildings.

A future work shall be focused on obtaining convective and radiative coefficients in rooms with a semitransparent wall with a selective solar control film in order to control solar radiation transmission. It will be necessary to investigate the flow patterns involved in turbulent three-dimensional situations. Although the extension to three dimensions is straightforward, the dramatic increase in CPU time is still a limitation in problems like the one here considered, where a large number of parameters are involved and many simulations have to be done.

## References

[1] G. De Vahl Davis, Natural convection of air in a square cavity: A benchmark numerical solution, Int. J. Num. Meth. Fluids 3 (1983) 249–264.

[2] N.C. Markatos, K.A. Pericleous, Laminar and turbulent natural convection in an enclosed cavity, Int. J. Heat Mass Transfer 27 (1984) 755–772.

[3] M. Hortmann, M. Peric, G. Scheuerer, Finite volume multigrid prediction of laminar natural convection: Benchmark solutions, Int. J. Num. Meth. Fluids 11 (1990) 189–207.

[4] G. Barakos, E. Mitsoulis, D. Assimacopoulos, Natural convection flow in a square cavity revisited: Laminar and turbulent models with wall functions, Int. J. Num. Meth. Fluids 18 (1994) 696–719.

[5] R.A.W.M. Henkes, C.J. Hoogendoorn, Comparison exercise for computations of turbulent natural convection in enclosures, Numer. Heat Transfer B 28 (1995) 59–78.

[6] D.W. Pepper, K.G.T. Hollands, Summary of benchmark numerical studies for 3-D natural convection in an air filled enclosure, Numer. Heat Transfer A 42 (2002) 1–11.

[7] C. Balaji, S.P. Venkateshan, Combined surface radiation and free convection in cavities, J. Thermophys. Heat Transfer 8 (1994) 373–376.

[8] N. Ramesh, S.P. Venkateshan, Effect of surface radiation on natural convection in a square enclosure, J. Thermophys. Heat Transfer 13 (1999) 299–301.

[9] K. Velusamy, T. Sundararajan, K. Seetharamu, Interaction effects between surface radiation and turbulent natural convection in square and rectangular enclosures, J. Heat Transfer 123 (2001) 1062–1070.

[10] K.S. Anil, K. Velusamy, C. Balaji, S.P. Venkateshan, Conjugate turbulent natural convection with surface radiation in air filled rectangular enclosures, Int. J. Heat Mass Transfer 50 (2007) 625–639.

[11] R. Alvarado, J. Xamán, J. Hinojosa, G. Álvarez, Interaction between natural convection and surface thermal radiation in tilted slender cavities, Int. J. Thermal Sciences 47 (2008) 355–368.

[12] M. Behnia, J.A. Rizes, G. De Vahl Davis, Combined radiation and natural convection in a cavity with a transparent wall and containing a non-participant fluid, Int. J. Num. Meth. Fluids 10 (1990) 305–3225.

[13] S.S. Kwon, Y.I. Kwon, J.L. Park, Numerical study of combined natural convection and radiation in a rectangular enclosure with a semitransparent window on the center region of right wall, in: 6th Int. Symposium on Transport Phenomena in Thermal Engineering, 1993, pp. 299–304.

[14] G. Álvarez, C.A. Estrada, Numerical heat transfer in a cavity with a solar control coating deposited to a vertical semitransparent wall, Int. J. Num. Meth. Fluids 34 (2000) 585–607.

[15] J. Xamán, G. Álvarez, Effect of heat conduction of SnS–$Cu_x$ solar control coated semitransparent wall on turbulent natural convection in a square cavity, Numer. Heat Transfer A 50 (2006) 79–98.

[16] R. Henkes, F. Van-Der-Vlugt, C. Hoogendoorn, Natural-convection flow in a square cavity calculated with low-Reynolds-number turbulence models, Int. J. Heat Mass Transfer 34 (1991) 377–388.

[17] M. Modest, Radiative Heat Transfer, McGraw-Hill, New York, 1993.

[18] S. Patankar, Numerical Heat Transfer and Fluid Flow, Hemisphere Publishing, Washington, 1980.

[19] J. Van Doormaal, G. Raithby, Enhancements of the SIMPLE method for predicting incompressible fluid flow, Numer. Heat Transfer 7 (1984) 147–163.